

QUARTERLY JOURNAL
OF THE
ROYAL METEOROLOGICAL SOCIETY

Vol. 114

OCTOBER 1988

No. 484

Q. J. R. Meteorol. Soc. (1988), **114**, pp. 1365–1384

551.524.735(215–13)

A study of the stratospheric final warming of 1982 in the southern hemisphere

By C. R. MECHOSO*, A. O'NEILL†, V. D. POPE† and J. D. FARRARA*

* *Department of Atmospheric Sciences, University of California, Los Angeles, U.S.A.*; † *Meteorological Office, Bracknell*

(Received 13 October 1987; revised 13 May 1988)

SUMMARY

The three-dimensional evolution of the final warming that takes place in the stratosphere of the southern hemisphere during spring is studied using data from a satellite. The event of spring 1982 is discussed in detail, and other events from an 8-year set are briefly surveyed. The zonal-mean westerly jet moves poleward and downward in spring as strong, planetary-scale disturbances develop which contribute to the weakening of the stratospheric westerly vortex. The processes governing this weakening are discussed by reference to isentropic maps of Ertel's potential vorticity and associated area diagnostics. The vortex breaks down first in the upper stratosphere and then later (and more slowly) in the middle stratosphere. This behaviour is broadly reproduced year after year. Repeating life-cycles of growth, eastward movement and decay of anticyclones in the stratosphere are described and related to the behaviour of quasi-stationary wave 1 and eastward-travelling wave 2. Evidence that the topography of the southern hemisphere exerts a strong influence on the evolution of the final warming is presented. An association is found between the location of anticyclones in the upper stratosphere, warm pools of air in the lower stratosphere and a climatological split of the westerly jet stream in the upper troposphere.

1. INTRODUCTION

The most dramatic dynamical events in the seasonal evolution of the stratosphere in the southern hemisphere occur during the final warming in spring. Strong planetary-scale disturbances develop, especially in September and October, which affect the radiative balance in the stratosphere and alter the distribution of temperature and winds. The westerly vortex becomes highly distorted and weakens steadily before breaking down rapidly in the upper stratosphere. The discovery of the springtime 'ozone hole' over Antarctica (Farman *et al.* 1985) gives impetus to dynamical studies of final warmings. The stratospheric circulation is bound to have a bearing on the evolution of the ozone hole.

In this paper, we use satellite data to give a comprehensive analysis of the final warming that took place in the stratosphere of the southern hemisphere during spring 1982, a case chosen because the flow was unusually disturbed but otherwise typical. To gain a broad view of the changes in the circulation, we describe the evolution of zonally averaged quantities (temperatures, winds, eddy amplitudes and fluxes). We then focus on how changes in these quantities are connected with changes (systematic and otherwise) on synoptic maps for the stratosphere and upper troposphere. Special attention is directed to a large-amplitude, quasi-stationary wave 1 and to an eastward travelling wave 2 in the stratosphere. We give a detailed, three-dimensional description of how the westerly vortex breaks down, discussing the radiative and dynamical processes at work, and give

evidence for a link between the stratospheric and tropospheric circulations. Finally, we compare the final warming in 1982 with that in 1981 (a somewhat less disturbed event), and illustrate inter-annual variability with time-mean maps for eight events.

Recent observational studies of final warmings in the southern hemisphere that have used satellite data include the following. Shiotani and Hirota (1985) included an examination of the final warming in the southern hemisphere in their study of the zonal-mean evolution of the stratosphere in both hemispheres from June 1981 to May 1982. They found that there was a downward shift in the stratosphere of the zonal-mean westerly jet core as the final warming progressed, and enhanced activity of wave 1. Yamazaki and Mechoso (1985) noted that the warming in 1979 was nearly monotonic but was modulated by episodes of enhanced planetary-wave activity, some of which could be traced down to the troposphere. Farrara and Mechoso (1986) and Mechoso and Farrara (1987) compiled a climatology and examined the inter-annual variability of final warmings in the southern hemisphere for the years 1978–1983. They showed that there is inter-annual variability in association with variability in planetary-wave activity. Yamazaki's (1987) comparison of final warmings in the two hemispheres was based mainly on transformed Eulerian mean diagnostics. He found that in 1982 the final warming in the southern hemisphere was more rapid and intense than it was in the northern hemisphere. He also found that the reversal of zonal-mean winds from westerly to easterly did not extend downwards as far into the lower stratosphere in the southern hemisphere as it did in the northern hemisphere.

The plan of this paper is as follows. In section 2 we describe the data used and method of analysis. Section 3 contains an account of the final warming in the southern hemisphere during spring 1982. An indication of inter-annual variability in the phenomenon is given in section 4, where we extend the climatology of Mechoso and Farrara by including data for more years. Our conclusions are listed in section 5.

2. DATA AND METHOD OF ANALYSIS

The data used here were obtained mainly from stratospheric sounding units (SSU, MSU and HIRS-2) on board the satellite NOAA-6 of the Tiros-N series. Details of data retrieval and a discussion of the errors involved are given by Clough *et al.* (1985) and references therein. In brief, the analysis proceeds as follows:

- (1) Radiances are inverted to give thicknesses by statistical regression.
- (2) The thicknesses are added to an analysis of geopotential height at 100 mb provided by the U.S. National Meteorological Center (NMC), giving geopotential heights at 20, 10, 5, 2 and 1 mb. An NMC analysis of geopotential height is included at 50 mb to augment the vertical resolution in the lower stratosphere; NMC analyses are also used for the troposphere.
- (3) Fields are smoothed by Fourier analysis with truncation at wavenumber 12 in the zonal and meridional (pole to pole) directions.
- (4) Winds are estimated using the geostrophic relation (fields of gradient winds are noisier).
- (5) Temperatures are calculated from geopotential heights by differentiating them in the vertical.
- (6) Ertel's potential vorticity is computed from the wind and temperature fields by using an approximation valid for small Rossby number and large Richardson number:

$$Q \sim -g(\xi_p + f)\partial\theta/\partial p \quad (1)$$

where the notation is detailed in the appendix.

As there are only a few radiosonde measurements in the southern hemisphere for the base height analysis at 100 mb, stratospheric analyses in the southern hemisphere are not as reliable as they are in the northern hemisphere. A preliminary assessment was made of the effect on stratospheric analyses of using different analyses for base height. This exercise formed part of a workshop on the inter-comparison of satellite data from different sources (Williamsburg, Virginia, U.S.A.; report in preparation edited by W. L. Grose and A. O'Neill). Base heights were obtained from three sources: the Meteorological Office; the NMC; and the European Centre for Medium Range Weather Forecasts. The three sets of stratospheric fields were mostly in broad qualitative agreement but there were significant quantitative differences, especially near the south pole. Qualitative reliability of analyses is adequate for this study.

3. STRATOSPHERIC FINAL WARMING IN THE SOUTHERN HEMISPHERE IN SPRING 1982

(a) *Evolution of zonal-mean quantities: winds, temperatures, eddy amplitudes*

A height–time section of zonal-mean temperature for late winter and spring averaged over the latitude band 70° to 80°S is shown in Fig. 1(a). There is a gradual and persistent warming over a deep layer of the stratosphere with maximum changes in temperature between 30 and 50 mb (near where stratospheric temperatures were lowest in early September). Superimposed on the general temperature trend are short-period warmings followed by coolings (e.g. at the end of September and in late October). The fastest rise in temperature is in the middle stratosphere (near 10 mb) in late October. Afterwards, temperatures fall in this region for most of November.

A latitude–time section of zonal-mean temperature at 10 mb is shown for the same period in Fig. 1(b). The latitudinal temperature gradient changes sign at this level in early October, but in the upper stratosphere the sign change has already occurred by the beginning of September.

The evolution of zonal-mean wind is shown in Fig. 2. Zonal-mean winds decelerate throughout the stratosphere at 60°S (Fig. 2(a)) for most of the period shown. The largest and most rapid changes are in the upper stratosphere, notably in late October when zonal-mean easterlies replace westerlies during a strong warming pulse (Fig. 1(b)). The westerly jet core then descends rapidly from the middle to the lower stratosphere and thereafter it descends more slowly. In the zonal-mean, easterlies replace westerlies only in the middle and upper stratosphere; in the lower stratosphere, winds remain westerly.

At 10 mb, zonal-mean easterlies first appear at low latitudes and then migrate polewards (Fig. 2(b)), whereas in the upper stratosphere, zonal-mean easterlies first appear at high latitudes (not shown). The westerly jet core moves downwards and polewards, as is characteristic of final warmings in the southern hemisphere (Hartmann 1976, and others). This movement occurs not only because the westerly vortex gets smaller, but also because it becomes increasingly asymmetric about the pole with height, as discussed below.

A height–time section of the upward component of the Eliassen–Palm flux is shown in Fig. 3. The warming pulses and accompanying wind decelerations happen in unison with bursts in the eddy flux. Sometimes these bursts are evident in the upper troposphere as well as in the stratosphere (two instances are marked by arrows on the figure). If the flux is taken to indicate the quasi-linear, vertical propagation of wave activity, a possible physical interpretation of this correspondence is that a disturbance originates in the troposphere and propagates upwards into the stratosphere. At other times, however, the troposphere and stratosphere do not seem to be connected in this way (two instances marked by crosses), even if allowance is made for a time delay of a few days for waves

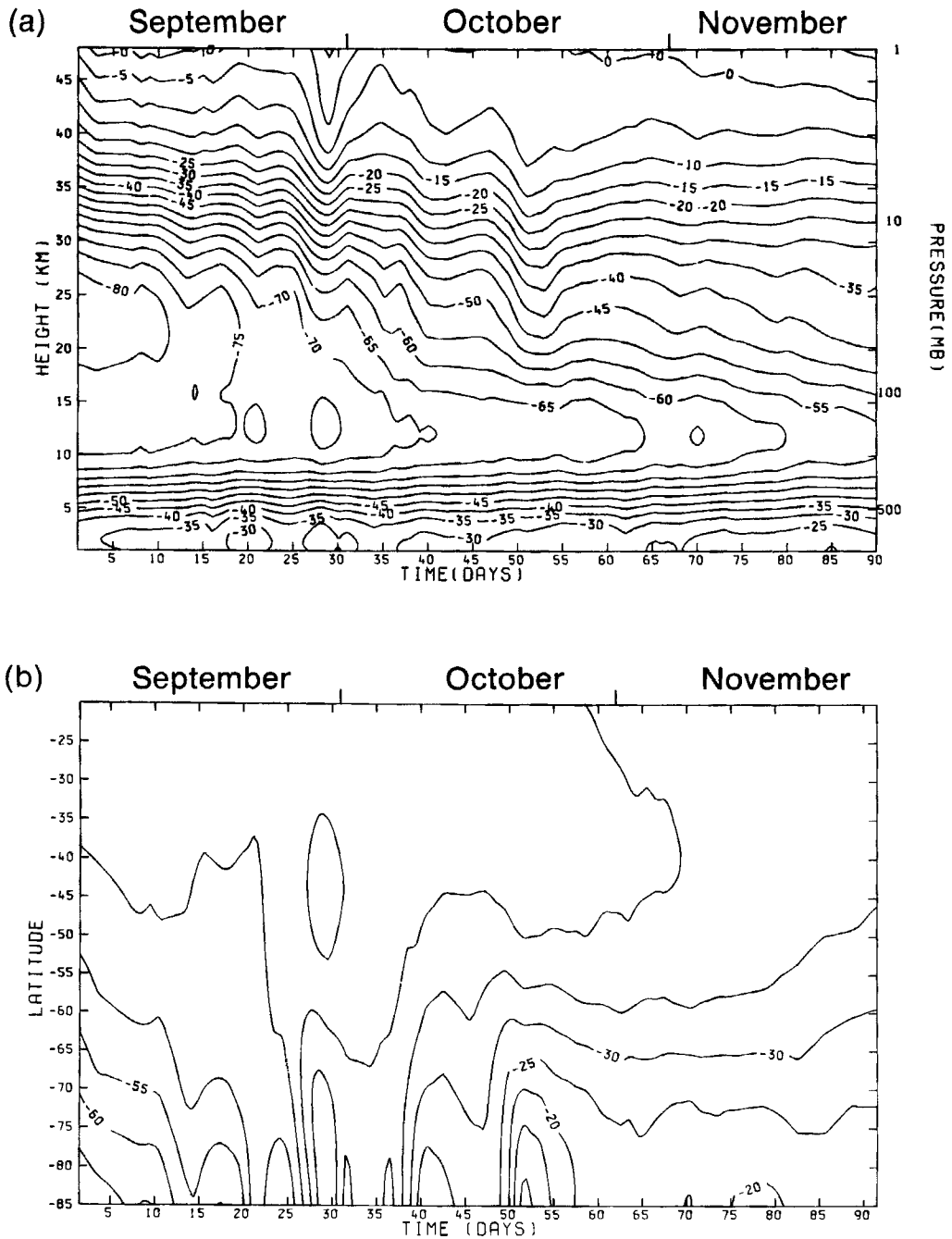


Figure 1. Variation of zonal-mean temperature from 1 September to 30 November 1982. The contour interval is 5 degC. (a) Height-time section averaged between 70°S and 80°S. (b) Latitude-time section at 10 mb.

to propagate upwards. Mechoso and Hartmann (1982) also found for the southern hemisphere that some eddy motions are not coherent between the troposphere and stratosphere, and suggested that nonlinearity could be one of a number of possible explanations for this. We give evidence supporting this idea later.

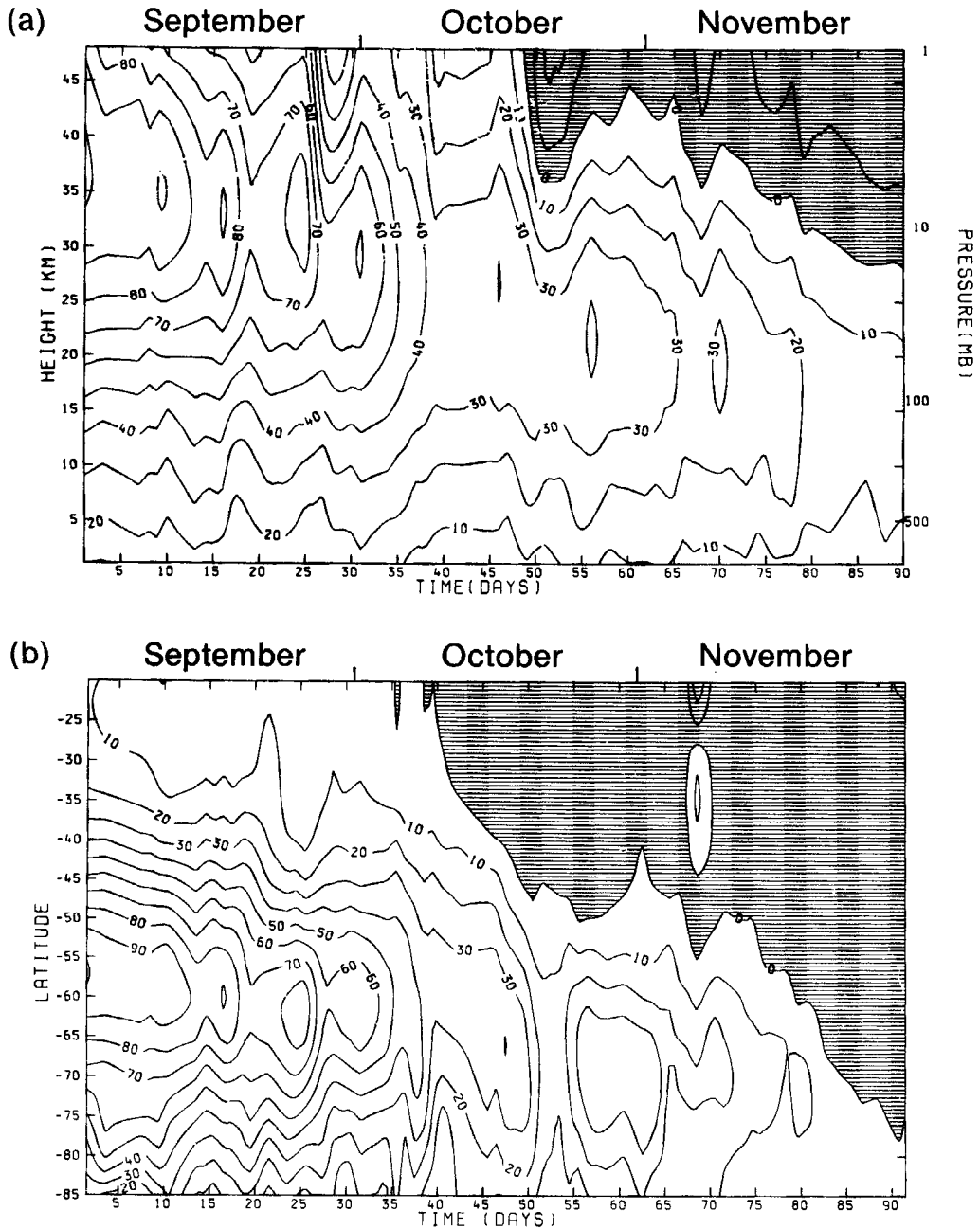


Figure 2. Variation of zonal-mean wind from 1 September to 30 November 1982. The contour interval is 10 m s^{-1} . Values less than zero are shaded. (a) Height-time section at 60°S . (b) Latitude-time section at 10 mb.

There are large eddy fluxes in the stratosphere for most of September and for the first half of October. Just after mid October, eddy fluxes fall rapidly in magnitude. Temperature variations around latitude circles become small as a pool of warm air moves over the polar region and becomes roughly symmetric about the pole (see discussion of Fig. 4).

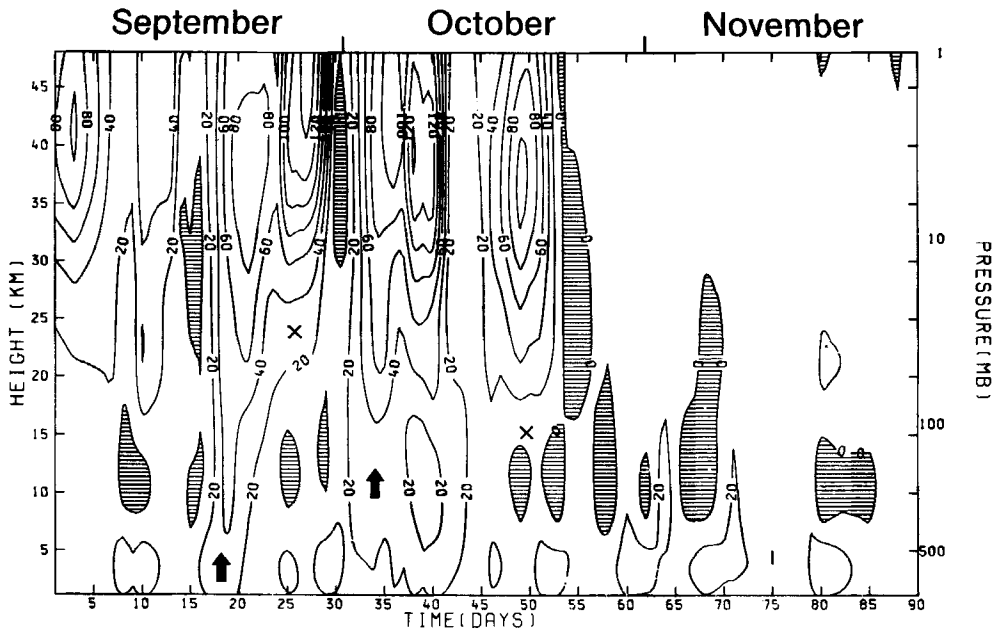


Figure 3. Height-time section from 1 September to 30 November 1982 of the vertical component of the Eliassen-Palm flux, $F_{(z)}$, averaged between 50°S and 70°S . $F_{(z)}$ is the quantity on the right-hand side of Eq. 2.2(b) in Dunkerton *et al.* (1981) multiplied (for scaling purposes) by the factor $1000/p$, where p is in mb. Units are $10^{12}\text{kg m s}^{-1}$. Arrows mark rapid increases in $F_{(z)}$ in the stratosphere that are apparently connected with increases in the troposphere; crosses mark instances when no such connection can be made.

(b) Synoptic description of the final warming

We begin by giving an outline of the synoptic evolution of the final warming, showing first how the temperature structure of the stratosphere changes, and second how the huge cyclonic vortex that characterizes the winter circulation is broken down.

A selection of maps of layer-mean (brightness) temperature for the middle and upper stratosphere is shown in Fig. 4. In the middle stratosphere in early September, (a), a large pool of cold air lies over the polar region with a smaller pool of warm air at low latitudes. There is a strong warming in early October, (b), and, by mid October, the cold pool disappears leaving the warmest air over the polar region, (c). This is consistent with the downward movement of the jet core in Fig. 2(a). In the upper stratosphere, the synoptic sequence is similar, (d), (e) and (f), but with warm air already over the polar region in early September.

Notice that the warming happens asymmetrically about the pole. This is typical of final warmings in the middle and upper stratosphere in the southern hemisphere, and indicates a significant dynamical element in the final warmings. In the eight years for which we have data (1979 to 1986), the final warming during spring in the southern hemisphere has a favoured geographical region – it always begins in the eastern half of the hemisphere. This geographical preference, already noted by Godson (1963), implies a topographic connection, as discussed further in section 3(d).

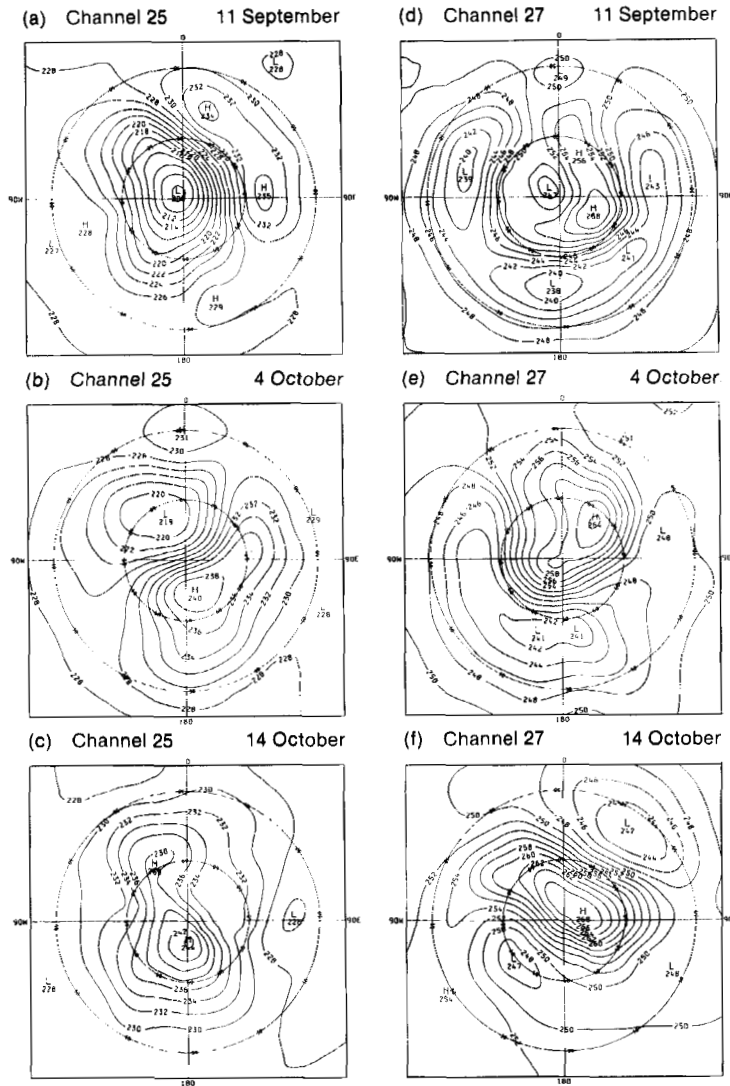


Figure 4. Polar-stereographic maps of brightness temperature for two channels of the SSU radiometer: channel 25, weighting function peaking at about 15 mb; channel 27, weighting function peaking at about 1.5 mb. The contour interval is 2 K. (a) 11 September, (b) 4 October and (c) 14 October 1982 for channel 25. (d), (e) and (f), the same dates for channel 27.

During the first half of September, a strong cyclone dominates the circulation throughout the stratosphere, as is shown by synoptic maps of geopotential height in Fig. 5(a). Shading highlights the area where gradients in geopotential height (and hence westerly winds) are strong. Notice that the shading covers a similar area at each level. By the third week of October, the structure of the cyclone has changed significantly, as indicated by the shaded areas in Fig. 5(b). The cyclone has shrunk, and this shrinkage increases with height; the shaded areas in Fig. 5(b) can be thought of as cross-sections of a distorted cone. These changes in the cyclone attend the development in the middle and upper stratosphere of a closed anticyclonic circulation.

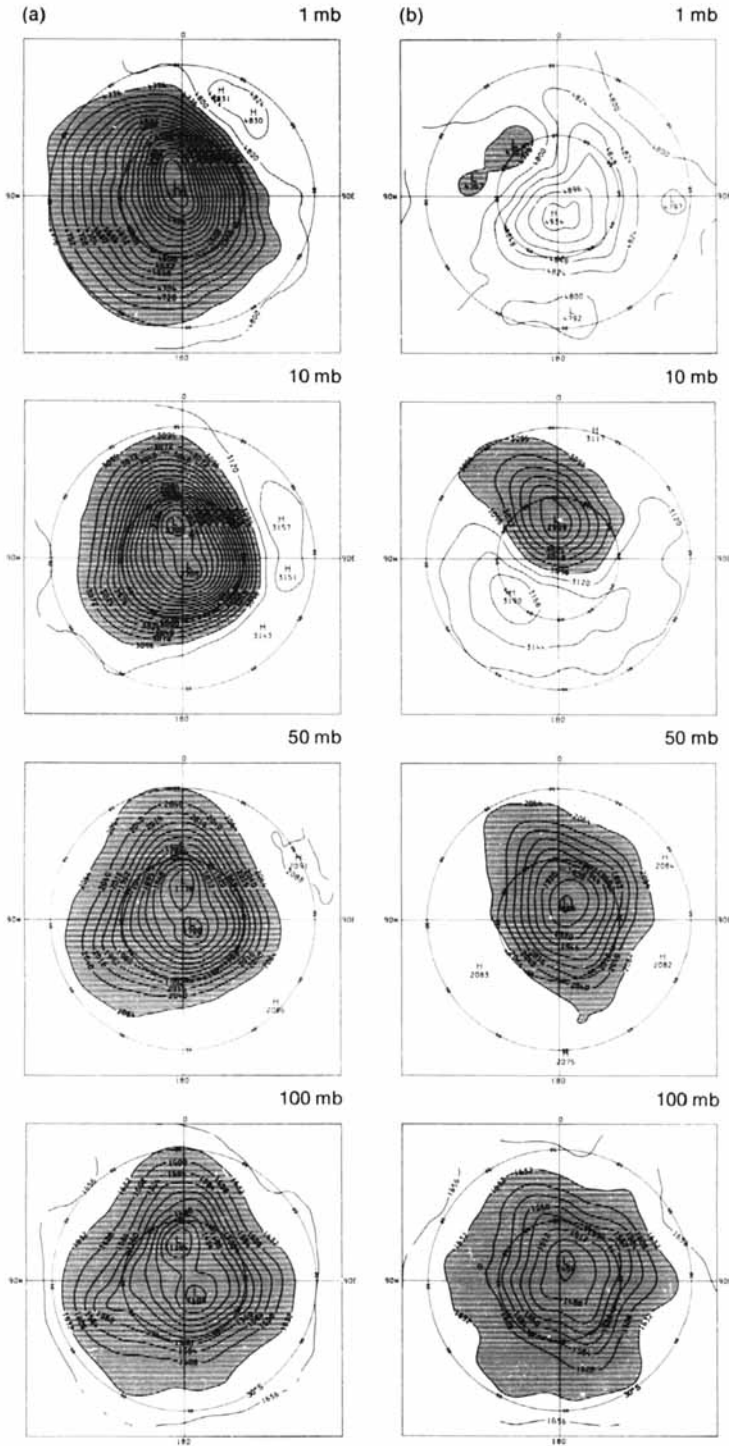


Figure 5. Polar-stereographic maps of geopotential height at 100, 50, 10 and 1 mb for (a) 11 September 1982, and (b) 21 October 1982. The contour interval is 24 dam. The shading roughly defines the area of strong cyclonic circulation. At a given level, the value of geopotential height used to delineate the edge of the shading is the same for both days.

We now study in more detail the evolution of the circulation during spring 1982. Three stages (not completely distinct) can be identified:

- (1) In September, the stratospheric flow is dominated at all levels by a large westerly vortex. On it are planetary-scale disturbances which travel eastward.
- (2) In October, disturbances are quasi-stationary. As amplitudes become large, the vortex breaks down in the upper stratosphere, and it shrinks more rapidly than before in the middle and lower stratosphere.
- (3) In November, the circulation is weak, and the residue of the westerly vortex gradually breaks down as summer radiation conditions approach.

(1) *September.* A sequence of synoptic maps of geopotential height at 10 mb for a selection of days in September is shown in Fig. 6. On 11 September, (a), there is a strong, slightly deformed cyclone lying over the polar region. The cyclone becomes elongated as an anticyclone builds near 60°E over the Indian Ocean, and the whole pattern rotates eastwards, (b) and (c) for 13 and 17 September, until the anticyclone finally decays near 240°E over the Pacific, (d) for 25 September.

The patterns shown in Fig. 6 extend through the middle and upper stratosphere with little westward tilt with height. In the lower stratosphere, zonal asymmetries are more apparent in the temperature field (not shown) than in the height field. An empirical finding is that the anticyclones at 10 mb lie directly above warm pools of air at 100 mb.

The life-cycle of growth, advection and decay shown in Fig. 6 is the middle one of a series of three similar developments in September 1982, each lasting about 10 days. As one anticyclone decays over the Pacific, another starts to build over the Indian Ocean (e.g. Fig. 6(d)), and it is then advected eastwards towards the Pacific. At high latitudes, the elongated cyclone rotates eastwards by about 180° during each life-cycle.

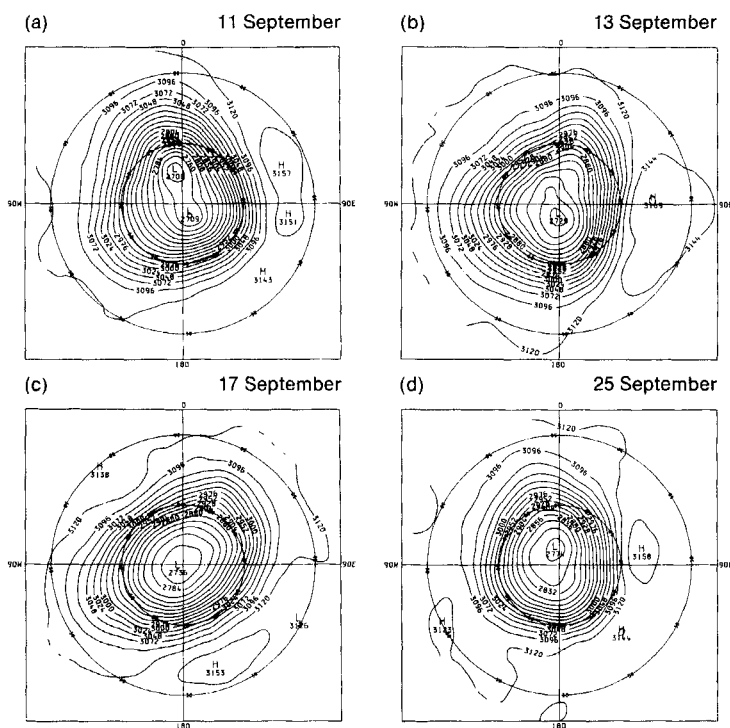


Figure 6. Polar-stereographic maps of geopotential height at 10 mb for (a) 11 September, (b) 13 September, (c) 17 September and (d) 25 September. The contour interval is 24 dam.

The eastward rotation of the height pattern is reflected in travelling zonal harmonics, most clearly in a large-amplitude, eastward-travelling wave 2 (associated at high latitudes with the elongated cyclone). Figure 7(a) shows the variation with time of the amplitude and phase of wave 2 at 60°S during September. The amplitude of wave 2 fluctuates with each cycle but there is a steady eastward phase speed of about 20° per day throughout the period shown.

More than one zonal harmonic is intimately linked with the synoptic evolution just described. The amplitude of wave 1 is similar to that of wave 2 but its phase changes are somewhat more complicated, as shown in Fig. 7(b). Arrows on the abscissa roughly mark the start of each life-cycle. The phase speed of wave 1 changes sign repeatedly as one anticyclone forms while another decays about 180° away in longitude, but the phase remains within the same quadrant.

We find that this synoptic sequence and associated behaviour of zonal harmonics is typical of other Septembers in the eight years for which we have data. Harwood (1975) and Leovy and Webster (1976) noted an eastward-travelling wave 2 and a quasi-stationary wave 1 in the stratosphere of the southern hemisphere during September 1971. No definitive explanation for the travelling wave 2 has yet been proposed, though Mechoso and Hartmann (1982) listed and discussed some possibilities. A theory for the travelling wave 2 would have to explain (1) its large vertical wavelength and barotropic structure in the stratosphere; (2) its intimate connection with wave 1 manifested by the life-cycle of a localized anticyclone; and (3) the geographical preference noted above.

(2) *October.* A sequence of synoptic maps of geopotential height at 10 mb for a selection of days in October is shown in Fig. 8. At the end of the third life-cycle in September 1982, the anticyclone does not decay once it is over the Pacific, as in earlier cases, but continues to develop there, (a), (b) and (c). The cyclone shrinks rapidly as the anticyclone builds (compare (b) and (c)), a process that is associated with the transfer of potential vorticity from one circulation system to the other (section 3(c) below). The anticyclone decays at the end of the month, by which time the cyclone has not been fully broken down; its residue is left over the polar region, (d). In the upper stratosphere, the breakdown is complete by about 22 October, as indicated by the zonal-mean winds (Fig. 2(a)). The synoptic evolution of the final warming described above is similar in many ways to that during strong minor and major warmings of the 'wave-1 type' in the northern hemisphere (compare Fig. 1(b) in McIntyre and Palmer (1983) with our Fig. 8(c)).

Once the anticyclone over the Pacific is strong in October, a second, weaker anticyclone starts to build about 180° away in longitude (Fig. 8(b)). Consistent with these synoptic developments, the amplitude of wave 2 increases while that of wave 1 decreases (not shown). The second anticyclone subsequently travels eastwards and merges with the one over the Pacific (Fig. 8(c)). The amplitude of wave 1 then increases again. Indirect evidence that such behaviour involves inherently nonlinear couplings of waves 1 and 2 comes from the work of O'Neill and Pope (1988). They found a similar sequence of events in idealized numerical experiments of strong disturbances in the stratosphere, and gave several pieces of evidence that the waves were coupled nonlinearly in the simulations. Wave amplitudes during the final warming studied here are comparable to those in the simulated flow. O'Neill and Pope noted that an anticorrelation in time of the amplitudes of waves 1 and 2 is a common feature of the circulation in the stratosphere of the northern hemisphere when disturbances are strong.

In the controlled conditions of O'Neill and Pope's experiment (the model had a prescribed lower boundary condition near the tropopause), fluctuations in wave amplitudes and associated changes in zonal-mean wind were not individually connected with

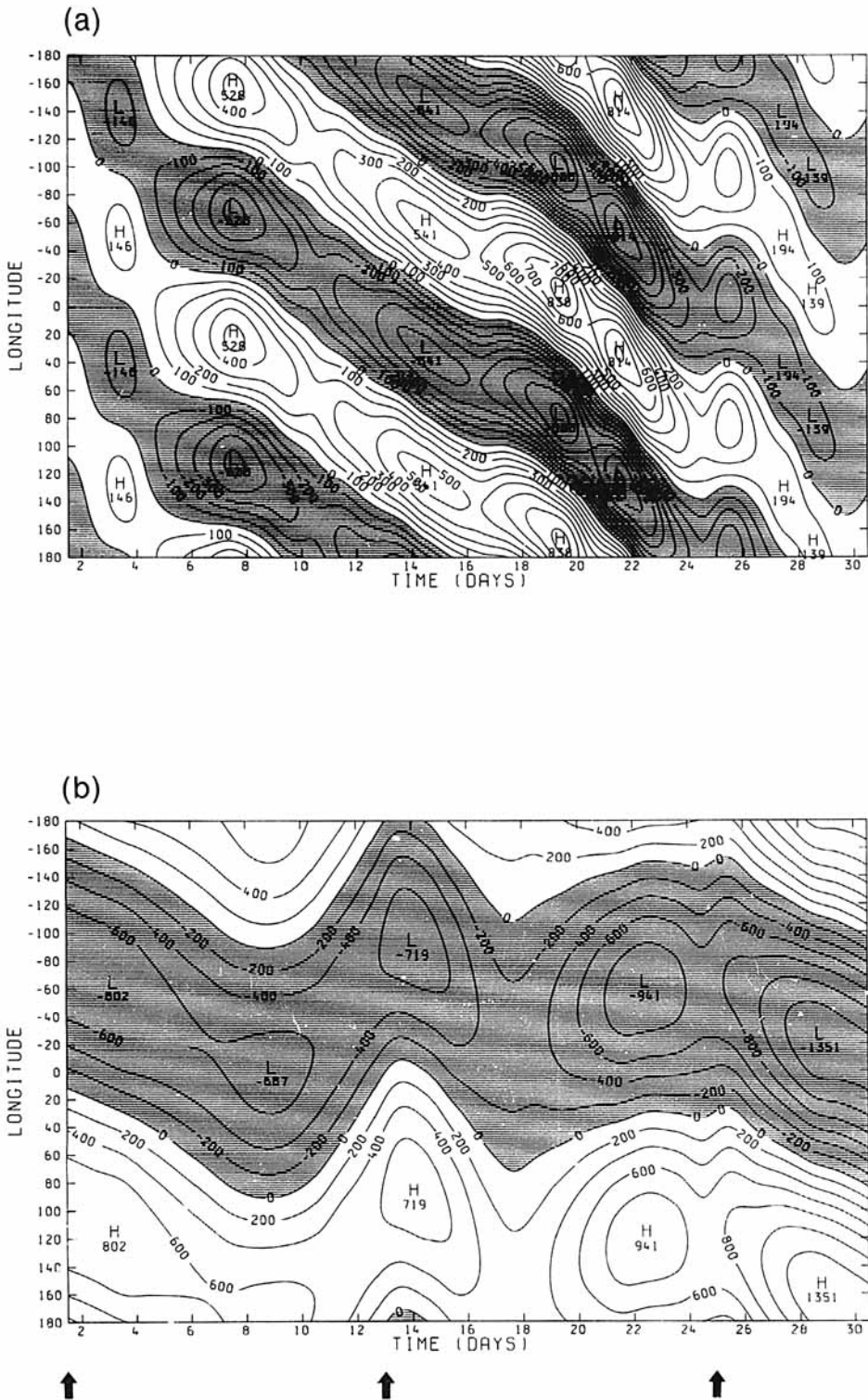


Figure 7. Longitude–time sections at 10 mb, 60°S of geopotential height from 1 September to 30 September 1982. The contour interval is 200 m. Negative values are shaded. (a) Wave-2 component, (b) wave-1 component. Arrows on abscissa mark start of life cycles, as described in the text.

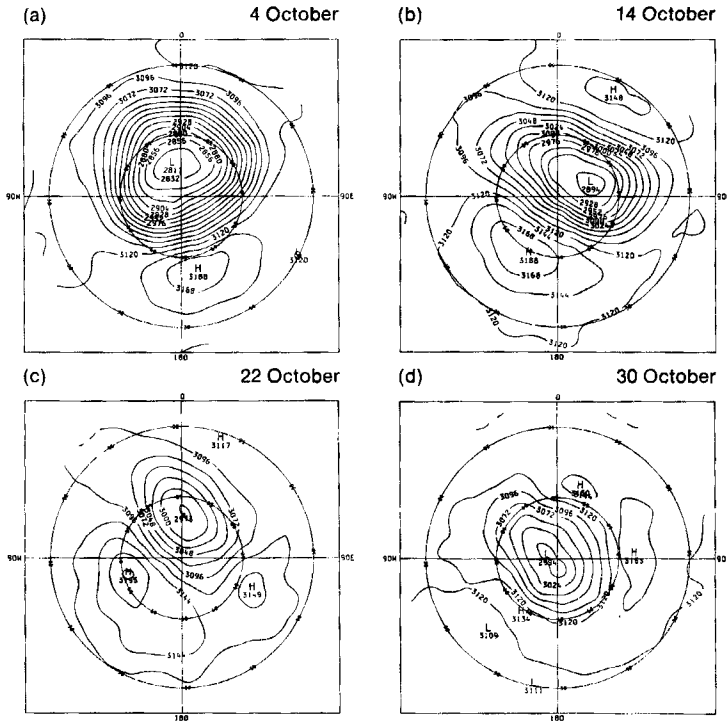


Figure 8. Polar-stereographic maps of geopotential height at 10 mb for (a) 4 October, (b) 14 October, (c) 22 October and (d) 30 October 1982. The contour interval is 24 dam.

pulsations in tropospheric forcing. Sudden bursts in the vertical component of the Eliassen–Palm flux, such as are indicated in Fig. 3, may result from nonlinearity internal to the stratosphere rather than from increased tropospheric forcing.

(3) *November.* During November in the middle stratosphere, maximum temperatures in the warm pool of air over the polar region increase slowly, presumably on account of radiative heating (the cooling shown in Fig. 1 is a product of zonal averaging). The small cyclone gradually weakens, to be replaced by a weak anticyclone by the end of the month. The cyclone also weakens slowly in the lower stratosphere, and towards the end of November its centre migrates to about 70°S over the S. Atlantic (about 30°W). At the end of the month, there are still westerly winds below about 20 mb (see Fig. 2(a)).

(c) *Material advection and systematic changes in potential vorticity*

Following from the invertibility principle (Hoskins *et al.* 1985), high values of Ertel's potential vorticity, Q , in a local area act as a source of cyclonic circulation; and low values a source of anticyclonic circulation (for the southern hemisphere, take 'high' and 'low' to refer to the modulus). The rapid shrinkage of the cyclone in the stratosphere during October is associated with the systematic drawing away of its high Q by a growing anticyclone.

The process is illustrated in Fig. 9(a), which is a map of Q and winds on the 850 K isentropic surface (near 10 mb) in mid October. The cyclone can be broadly identified with strong Q gradients. In the bottom left quadrant of the figure, there is a vigorous anticyclonic circulation where Q gradients are much weaker, and around which is stretched a tongue of relatively high Q . The pattern of Q shown in the figure is, according

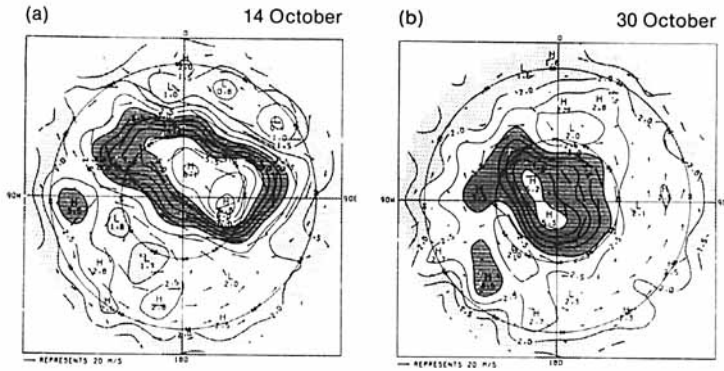


Figure 9. Polar-stereographic maps of the modulus of Ertel's potential vorticity on the 850 K isentropic surface for (a) 14 October and (b) 30 October. The contour interval is 0.5 in units of $10^{-4} \text{K m}^2 \text{kg}^{-1}$. In these units, heavy shading denotes values between 5 and 3, light shading values between 2 and 1.

to McIntyre and Palmer (1983, 1984, 1985), associated with the phenomenon of Rossby wave breaking, during which otherwise wavy Q contours (approximately material lines) are deformed irreversibly. Examples of the phenomenon in the stratosphere of the southern hemisphere have been reported by Al-Ajmi *et al.* (1985) and Newman (1986); an illustration from a high-resolution barotropic model has been presented by Juckes and McIntyre (1987).

The map of Q and winds at the end of October is shown in Fig. 9(b). The area where Q gradients are strong is much smaller than it was in mid October. Correspondingly, the area surrounding it where gradients are weak has increased. The shrinkage is not solely due to material advection on an isentropic surface. Notice that values of the modulus of Q are lower at the centre of the cyclone in Fig. 9(b) than they are in Fig. 9(a). This decrease illustrates the systematic reduction in maximum values of Q that takes place throughout spring. There is no indication from our analyses that air in the innermost portion of the cyclone is advected away. It is likely, therefore, that this systematic change (as distinct from the random, day-to-day variations that are found) is due to radiation.

Systematic changes in the structure of the circulation in the stratosphere during the final warming are conveniently summarized by plotting, for several values of Q , the variation in time of the area of an isentropic surface, $A(Q)$, where potential vorticity is greater than Q . This procedure has been used, for example, by Butchart and Remsberg (1986). One advantage of the area diagnostic is that it is coordinate independent, exposing systematic trends more clearly than do zonal-mean quantities. Another advantage is that changes in area can be directly related to non-conservative processes if the large-scale flow is approximately non-divergent (Butchart and Remsberg).

The variation in time of $A(Q)$ for the 850 K isentropic surface in the southern hemisphere during spring is shown in Fig. 10. Curves are plotted at equal intervals of Q and labelled with a value of Q in the units given in the figure legend. At a given time, the size of the cyclone in the stratosphere is given roughly by the value of $A(Q)$ at which there is a sharp change in the gradient, $dA(Q)/dQ$ (McIntyre and Palmer 1984). According to Fig. 10, this size is given by $A(3)$ during September and October (notice that the contour labelled '3' roughly encloses the cyclone in Fig. 9).

The cyclone shrinks steadily during September and October ($A(3)$ decreases), and there is an accompanying increase in the area where the gradient of Q is weak (curves labelled '2' and '3' separate with time). This would happen to some extent even in an

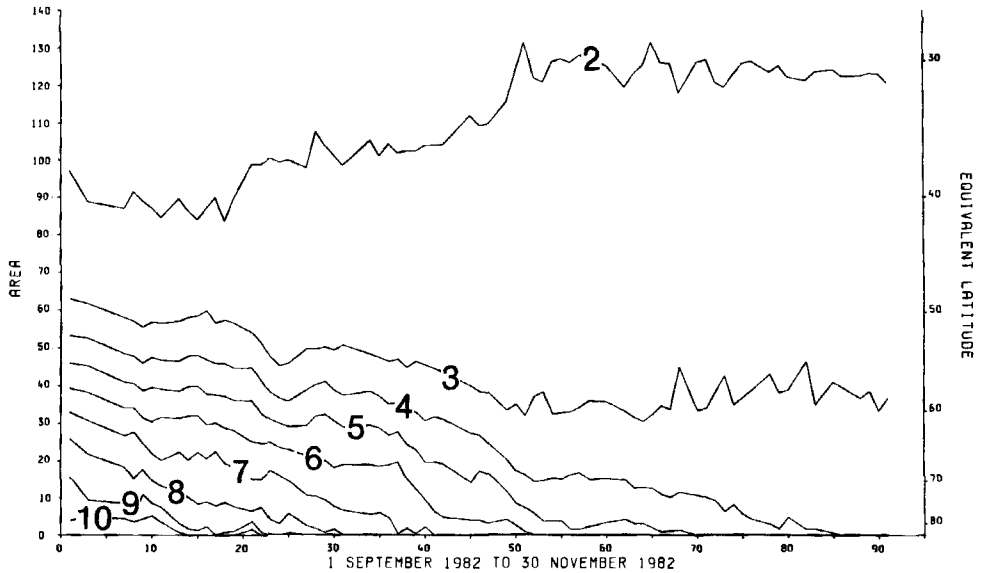


Figure 10. Graphs from 1 September to 30 November 1982 of the areas, $A(Q)$, where Q is greater than specified values on the 850 K isentropic surface. The units of area are 10^6 km^2 . Each graph is labelled with a value of Q in the units used in Fig. 9.

axisymmetric circulation because of the seasonal cycle in solar heating (Butchart and Remsberg 1986, Fig. 6). Planetary-scale disturbances lead to two additional effects which contribute to the shrinkage of the cyclone as measured by $A(Q)$ and to the weakening of the average gradient of Q around it:

(1) *Dynamically induced departures from radiative equilibrium.* Calculations show (O'Neill and Pope, paper in preparation) that radiation acts broadly to reduce variations in Q around latitude circles in the stratosphere. In the flow shown in Fig. 9(a), radiation would reduce high values of Q in the cyclone and increase low values in the anticyclone. Corresponding curves of $A(Q)$ separate with time, as in Fig. 10.

(2) *The generation of scales of motion too small to be fully resolved by the analysis.* McIntyre and Palmer (1983, 1984) suggested that the irreversible mixing of high and low Q (possibly taking place as the tongue of high Q in Fig. 9(a) is drawn out) would lead to changes in $A(Q)$ similar to those shown in Fig. 10.

The relative importance of processes (1) and (2) in the southern hemisphere has yet to be determined.

(d) *Link between final warming and circulation in upper troposphere*

Three pieces of evidence that the stratospheric circulation during the final warming in the southern hemisphere is governed to a significant extent from below are as follows:

- (1) During September, anticyclones develop in the stratosphere over a preferred geographical region.
- (2) During October, the anticyclone that precipitates the breakdown of the westerly circulation in the stratosphere is quasi-stationary.
- (3) Year after year, the final warming starts to develop in or near the same longitudinal quadrant, as shown in the next section.

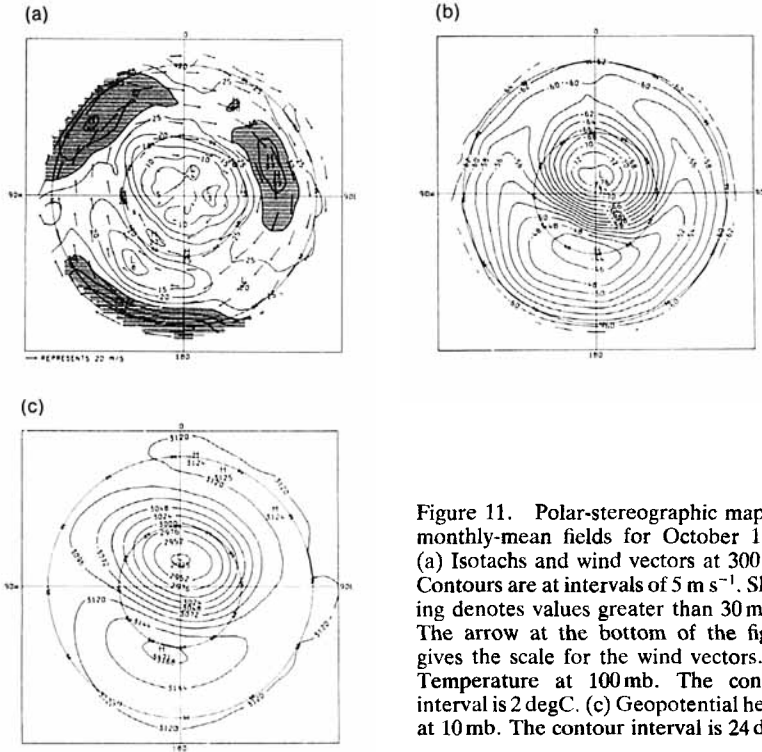


Figure 11. Polar-stereographic maps of monthly-mean fields for October 1982. (a) Isotachs and wind vectors at 300 mb. Contours are at intervals of 5 m s^{-1} . Shading denotes values greater than 30 m s^{-1} . The arrow at the bottom of the figure gives the scale for the wind vectors. (b) Temperature at 100 mb. The contour interval is 2 degC . (c) Geopotential height at 10 mb. The contour interval is 24 dam .

We shall illustrate an apparent connection between the circulations in the stratosphere and upper troposphere with monthly-mean maps for October 1982. During September, synoptic patterns are mobile in the stratosphere, and their connection with quasi-stationary features of the tropospheric circulation is less clear than it is during October.

Asymmetries in the tropospheric flow field in the southern hemisphere are well exposed by using maps of isotachs. The monthly-mean map of isotachs and wind vectors at 300 mb for October is shown in Fig. 11(a). The salient feature is the split in the westerly jet near the dateline: the strong jet at 90°E divides into a strong subtropical jet and a weaker jet that skirts Antarctica. Consistent with these synoptic features is the double jet structure in tropospheric zonal-mean winds found by Yamazaki (1987) shortly before a final warming. The split jet is a climatological feature of the upper troposphere in winter (e.g. James and Anderson 1984). On the basis of results from a simplified numerical model, James (1988) concluded that it is strongly linked to the zonal asymmetry of Antarctica.

This asymmetry in the wind field is reflected in a strong asymmetry in the temperature field in the lower stratosphere. The monthly-mean temperature at 100 mb for October is shown in Fig. 11(b). There is a pool of warm air at middle latitudes roughly above the region where winds are weak between the two tropospheric jets, and directly below the anticyclone in the monthly-mean geopotential height field at 10 mb (Fig. 11(c)).

We conclude therefore that the wave-1 character of the stratospheric final warming in the southern hemisphere is ultimately connected with the zonal asymmetry of the topography there.

4. INTER-ANNUAL VARIABILITY

A full analysis of the inter-annual variability of final warmings in the southern hemisphere warrants a separate study and is beyond our present scope. We give here a brief survey of the final warming of 1981, and of other final warmings in the years 1979 to 1986, to illustrate the type of variability found and to pick out some of the annually recurring features of the stratospheric flow.

Figure 12 shows monthly-mean maps for October 1981 corresponding to those shown for 1982 in Fig. 11. The mean features of the circulation in 1982 are also present in 1981 (and in other years): the split jet in the upper troposphere; the 'wave-1' asymmetry in temperature in the lower stratosphere; and the matching asymmetry in geopotential height in the middle stratosphere.

Stratospheric disturbances in October 1981 are weaker than those in 1982, and accordingly the westerly circulation takes longer to break down by the processes discussed in section 3(c). In the upper stratosphere, zonal-mean easterlies first appear in November, about two weeks later than they do in 1982. This difference seems to be connected with inter-annual variability in the troposphere. In particular, the split in the jet is less pronounced in 1981 than it is in 1982 (near the dateline, meridional gradients in wind speed are smaller in Fig. 12(a) than they are in Fig. 11(a)). There is a longitudinal shift of about 90° in stratospheric fields between the two years whose origin is unclear. The shift is not connected with a simple rotation of pattern in the troposphere.

Monthly-mean maps of geopotential height at 10 mb for Octobers from 1979 to 1986 are shown in Fig. 13. Though there is some inter-annual variability (the QBO may be a contributory factor (Garcia and Solomon 1987)), the broad pattern is much the same from one year to the next. In the monthly mean, the cyclone is roughly the same size and the attendant circulation roughly the same strength in the eight cases shown. There

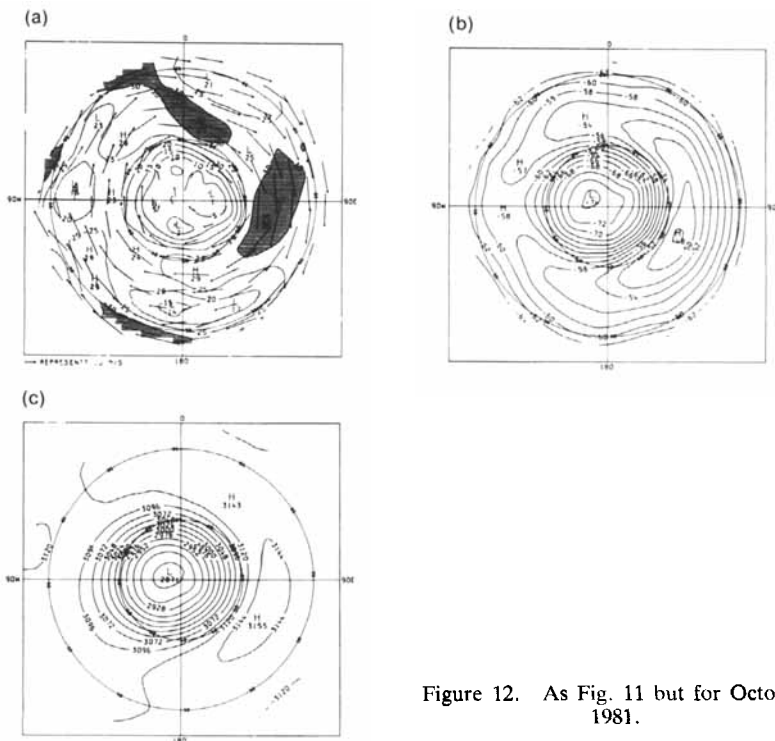


Figure 12. As Fig. 11 but for October 1981.

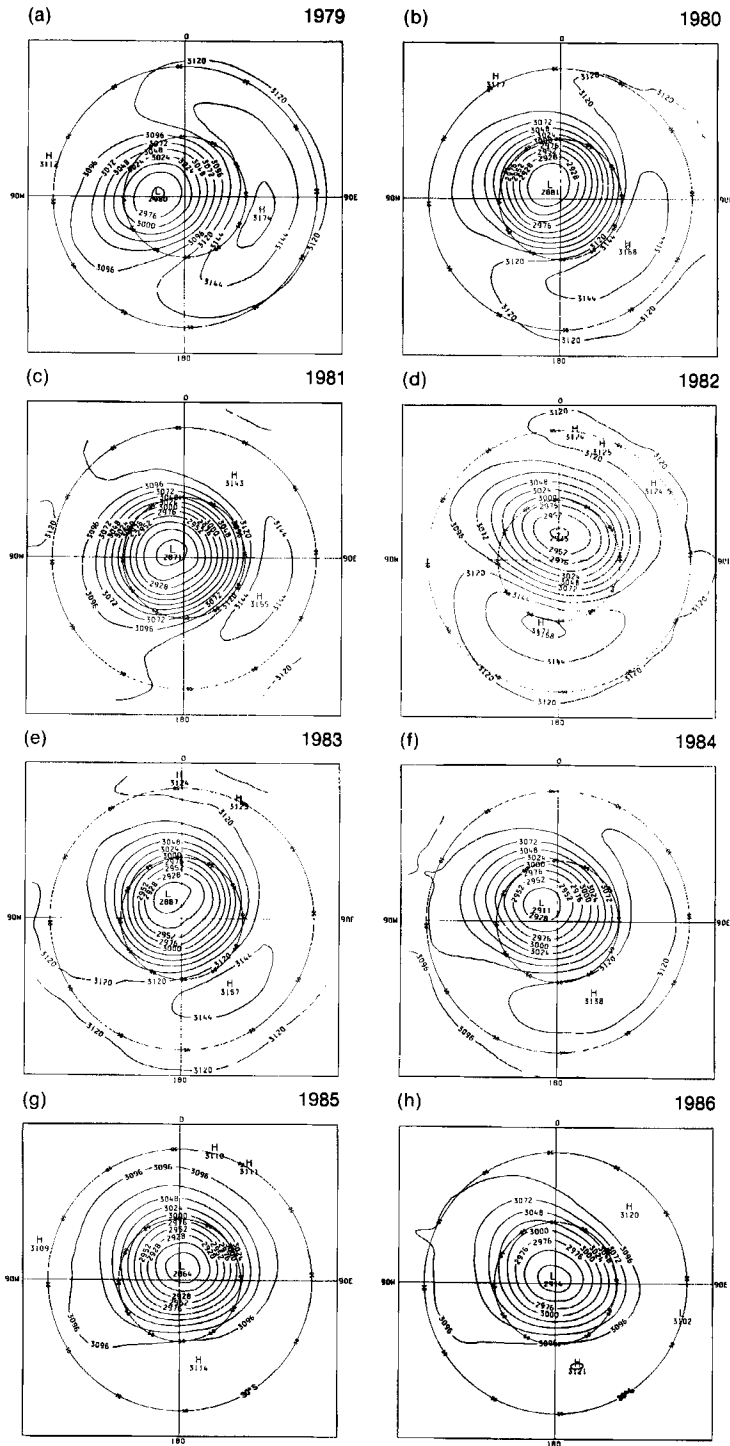


Figure 13. Polar-stereographic maps of monthly-mean geopotential height at 10 mb for October, 1979 to 1986. The contour interval is 24 dam.

is more noticeable variability in the intensity of the anticyclone: it was comparatively strong in 1979 and 1982, and somewhat weaker in 1985 and 1986. Correspondingly, the reversal of zonal-mean winds at mid-latitudes in the upper stratosphere was about two weeks earlier in the first pair of years. For each of the years shown, the anticyclone that persists in the middle stratosphere in October is always found roughly in the quadrant 90°E to 180°E , and the cyclone in the quadrant 0°W and 90°W . This is strong evidence for a topographic connection.

5. CONCLUSIONS

We study the three-dimensional evolution of the final warming that takes place in the stratosphere of the southern hemisphere during spring. Our broad aims are (1) to relate zonal-mean and synoptic views of the event; (2) to identify systematic changes in the circulation and to suggest possible causes; (3) to present evidence for links between the stratosphere and troposphere during the event; and (4) to give an indication of inter-annual variability. For these purposes, we examine the final warming of 1982 in detail, and give a brief survey of other cases from the eight years for which we have data.

In the stratosphere of the southern hemisphere during spring 1982, the zonal-mean jet decelerates as it moves downwards and polewards. Such behaviour is typical of final warmings in the southern hemisphere. The jet does not decelerate uniformly; rapid decelerations attend episodes of enhanced eddy fluxes in the stratosphere. Some of these cannot be associated with increased eddy activity in the troposphere, which points to the importance of nonlinear dynamics. Zonal-mean easterlies eventually appear in the upper stratosphere in mid October as the cyclone is displaced from the pole and rapidly broken down.

The final warming involves strong planetary-scale disturbances. During the early part of the warming, they comprise transient anticyclones which travel eastwards around a strong, elongated cyclone. We relate the repeating life cycles of these disturbances to an eastward-travelling wave 2 and to a quasi-stationary wave 1. Later in the warming, an intense, quasi-stationary anticyclone develops and persists. An anticorrelation in time between the amplitudes of waves 1 and 2 is a further indication of nonlinearity in the flow. We attribute the accompanying rapid shrinkage of the cyclone to the combined effects of the drawing away of its high potential vorticity by the growing anticyclone, and to dynamically induced radiative effects (over and above radiative effects that would exist in the seasonal cycle of a hypothetical, axisymmetric stratosphere). We find that the anticyclones in the middle stratosphere at 10 mb lie directly above warm pools of air in the lower stratosphere at 100 mb.

There is persuasive evidence that the topography of the southern hemisphere exerts a strong influence on the evolution of the final warming. In the spring of 1982, both travelling and quasi-stationary anticyclones formed over a preferred geographical region – the Indian Ocean. In every October of our 8-year set, the monthly-mean position of the quasi-stationary anticyclone in the middle stratosphere lies roughly between 90°E and 180°E . In this region is a climatological split in the tropospheric westerly jet stream, with an overlying warm pool of air in the lower stratosphere.

Although there is some inter-annual variability in the final warming, the synoptic evolution is broadly similar in each of our eight events: a strong anticyclone develops in the stratosphere over a preferred geographical area; the cyclone distorts, moves somewhat off the south pole, and breaks down first in the upper stratosphere and then later (and more slowly) in the middle stratosphere.

Such a predictable system is ideally suited for testing numerical models and dynamical theory of the atmosphere.

ACKNOWLEDGMENTS

We thank Michael McIntyre for his helpful comments on this paper. Betty Kingston prepared the figures. The research at UCLA was supported by NASA under grant NAGW-1021. Additional support was provided by a NATO grant for collaborative research.

APPENDIX

f	Coriolis parameter
g	Acceleration due to gravity
p	Pressure
Q	Ertel's potential vorticity
$A(Q)$	Area of an isentropic surface where potential vorticity $> Q$
T	Temperature
v	Meridional velocity
ζ_p	Relative vorticity on an isobaric surface
θ	Potential temperature

REFERENCES

- | | | |
|--|------|--|
| Al-Ajmi, D. N., Harwood, R. S. and Miles, T. | 1985 | A sudden warming in the middle atmosphere of the southern hemisphere. <i>Q. J. R. Meteorol. Soc.</i> , 111 , 359–389 |
| Butchart, N. and Remsberg, E. E. | 1986 | The area of the stratospheric polar vortex as a diagnostic for tracer transport on an isentropic surface. <i>J. Atmos. Sci.</i> , 43 , 1319–1339 |
| Clough, S. A., Grahame, N. S. and O'Neill, A. | 1985 | Potential vorticity in the stratosphere derived using data from satellites. <i>Q. J. R. Meteorol. Soc.</i> , 111 , 335–358 |
| Dunkerton, T., Hsu, C.-P. F. and McIntyre, M. E. | 1981 | Some Eulerian and Lagrangian diagnostics for a model stratospheric warming. <i>J. Atmos. Sci.</i> , 38 , 819–843 |
| Farman, J. C., Gardiner, B. G. and Shanklin, J. D. | 1985 | Large losses of total ozone in Antarctica reveal seasonal ClO_x/NO_x interaction. <i>Nature</i> , 315 , 207–210 |
| Farrara, J. D. and Mechoso, C. R. | 1986 | An observational study of the final warming in the southern hemisphere stratosphere. <i>Geophys. Res. Lett.</i> , 13 , 1232–1235 |
| Garcia, R. R. and Solomon, S. | 1987 | A possible relationship between inter-annual variability in Antarctic ozone and the quasi-biennial oscillation. <i>ibid.</i> , 14 , 848–851 |
| Godson, W. L. | 1963 | A comparison of middle stratosphere behaviour in the Arctic and Antarctic, with special reference to final warmings. <i>Meteorol. Abhandl.</i> , 36 , 161–206 |
| Hartmann, D. L. | 1976 | The structure of the stratosphere in the southern hemisphere during late winter 1973 as observed by satellite. <i>J. Atmos. Sci.</i> , 33 , 1141–1154 |
| Harwood, R. S. | 1975 | The temperature structure of the southern hemisphere stratosphere, August–October, 1971. <i>Q. J. R. Meteorol. Soc.</i> , 101 , 75–92 |
| Hoskins, B. J., McIntyre, M. E. and Robertson, A. W. | 1985 | On the use and significance of isentropic potential vorticity maps. <i>ibid.</i> , 111 , 877–946 |
| James, I. N. | 1988 | On the forcing of planetary scale Rossby waves by Antarctica. <i>ibid.</i> , 114 , 619–637 |
| James, I. N. and Anderson, D. L. T. | 1984 | The seasonal mean flow and distribution of large-scale weather systems in the Southern Hemisphere. <i>ibid.</i> , 110 , 943–966 |
| Juckes, M. N. and McIntyre, M. E. | 1987 | A high-resolution one-layer model of breaking planetary waves in the stratosphere. <i>Nature</i> , 328 , 590–596 |
| Leovy, C. B. and Webster, P. J. | 1976 | Stratospheric long waves: comparison of thermal structure in the Northern and Southern Hemispheres. <i>J. Atmos. Sci.</i> , 33 , 1624–1638 |

- McIntyre, M. E. and Palmer, T. N. 1983 Breaking planetary waves in the stratosphere. *Nature*, **305**, 593–600
- 1984 The 'surf zone' in the stratosphere. *J. Atmos. Terr. Phys.*, **46**, 825–849
- 1985 A note on the general concept of wave breaking for Rossby and gravity waves. *Pageoph*, **123**, 964–975
- Mechoso, C. R. and Farrara, J. D. 1987 'Climatology and interannual variability of wave, mean-flow interaction during winter and spring in the southern hemisphere'. Pp. 304–307 in preprints Second International Conference on Southern Hemisphere Meteorology, Wellington, New Zealand, December 1986. American Meteorological Society
- Mechoso, C. R. and Hartmann, D. L. 1982 An observational study of travelling planetary waves in the southern hemisphere. *J. Atmos. Sci.*, **39**, 1921–1935
- Newman, P. A. 1986 The final warming and polar vortex disappearance during the southern hemisphere spring. *Geophys. Res. Lett.*, **13**, 1228–1231
- O'Neill, A. and Pope, V. D. 1988 Simulations of linear and nonlinear disturbances in the stratosphere. *Q. J. R. Meteorol. Soc.*, **114**, 1063–1110
- Shiotani, M. and Hirota, I. 1985 Planetary wave–mean flow interaction in the stratosphere: A comparison between the northern and southern hemispheres. *ibid.*, **111**, 309–334
- Yamazaki, K. 1987 Observations of stratospheric final warmings in the two hemispheres. *J. Meteorol. Soc. Jap.*, **65**, 51–65
- Yamazaki, K. and Mechoso, C. R. 1985 Observations of the final warming in the stratosphere of the Southern Hemisphere during 1979. *J. Atmos. Sci.*, **42**, 1198–1205